Kaur and Singh *International Journal of Mechanical and Materials Engineering* (2021) 16:14
https://doi.org/10.1186/s40712-021-00137-3

International Journal of Mechanical and Materials Engineering

ORIGINAL PAPER　Open Access

Plane wave in non-local semiconducting rotating media with Hall effect and three-phase lag fractional order heat transfer

Iqbal Kaur[1*] and Kulvinder Singh[2]

Abstract

This paper deals with the propagation of the plane wave in a nonlocal magneto-thermoelastic semiconductor solid with rotation. The fractional-order three-phase lag theory of thermoelasticity with two temperatures has been applied. When a longitudinal wave is incident on the surface $z = 0$, four types of reflected coupled longitudinal waves (the coupled longitudinal displacement wave, the coupled thermal wave, coupled carrier density wave, and coupled transverse displacement wave) are identified. The plane wave characteristics such as phase velocities, specific loss, attenuation coefficient, and penetration depth of various reflected waves are computed. The effects of two temperatures, non-local parameter, fractional order parameter, and Hall current on these wave characteristics are illustrated graphically with the use of MATLAB software.

Keywords: Semiconducting media, Nonlocal, Hall current, Fractional-order derivative, Two temperatures

Introduction

The plane wave propagation in a photo-thermo-magneto-elastic solid has gained significant importance due to its applications in the area of semiconductors, magnetometers, solar panels, nuclear fields, geophysics, and other linked topics. Lotfy et al. (2020) discussed Hall current effect in a semiconductor medium exposed to a very strong magnetic field. Lotfy (2017) examined the wave propagation in a semiconductor medium having a spherical cavity using FOT. Ali et al. (2020) examined the reflection of waves over a semiconductor rotating medium using the TPL model with FOT. Tang and Song (2018) studied wave reflection in nonlocal semi-conductor rotating media by using the plasma diffusion equation. Alshaikh (2020) examined the transmission of photo-thermal waves in a semiconductor for diffusion and rotation effects. Kaur et al. (2020a) discussed the propagation of the plane wave in a visco-thermoelastic rotating medium with Hall current. Lata et al. (2021) discussed the propagation of plane harmonic waves thermo-magneto-elastic rotating medium with multi-dual-phase lag heat transfer. Lata and Kaur (2018) discussed the effect of Hall current on a rotating transversely isotropic thermoelastic medium with 2T. Eringen (2004; 1974; 1972) developed the nonlocal continuum mechanics theory to study the micro-scaled/nano-scaled structure problems. These theories exhibit that "consider the state of stress at a point as a function of the states of the strain of all points in the medium. But in classical continuum mechanics, the state of stress at a certain point uniquely depends on the state of strain on that same point". Also, some other researchers worked on the wave propagation in different media using different theories of thermoelasticity as Lim et al.(1992), Marin (2010; 1996), Abbas and Marin (2018), Kaur et al. (2020b; 2019a), Bhatti et al. (2019; 2020), Marin et al. (2015, 2016, 2020), Zhang et al. (2020a), Bhatti et al. (2021), Lata and Kaur (2019b; 2020; 2019), Pandey et al. (2021), Taye et al. (2021), Zhang et al. (2020b), Bhatti and Abdelsalam (2020), Zhang et al. (2021), and

* Correspondence: bawahanda@gmail.com
[1]Department of Mathematics, Government College for Girls, Palwal, Kurukshetra, Haryana, India
Full list of author information is available at the end of the article

Golewski (2021). Despite the above research, no research has been done for the plane wave propagation with the fractional order three-phase lag two-temperature heat transfer in rotating magneto thermoelastic nonlocal semiconducting medium.

This research investigates the transmission of plane waves in a nonlocal semiconducting rotating medium under the influence of a high magnetic field and Hall current. The governing equations are expressed with TPL-2T FOT of thermoelasticity. For considered 2-D model, when a longitudinal wave is incident on the surface z=0, four types of reflected waves distinguished as coupled longitudinal waves (CLD-wave, CT-wave, CCD-wave, CTD-wave) are identified. The plane wave characteristics of various reflected waves are computed numerically and demonstrated graphically. The effects of two temperatures, non-local parameter, fractional order parameter, and Hall current on wave characteristics illustrated graphically with the use of MATLAB software have been studied.

Basic equations

Following Tang and Song (2018), Othman and Abd-Elaziz (2019), and Mahdy et al. (2020), the equations of motion with Lorentz force is

$$\sigma_{ij,j} + \left(1-\epsilon^2\nabla^2\right)\mu_0\varepsilon_{ijr}J_jH_r = \rho\left(1-\epsilon^2\nabla^2\right)\left\{\ddot{u}_i + 2(\boldsymbol{\Omega}\times\dot{\boldsymbol{u}})_i + (\boldsymbol{\Omega}\times(\boldsymbol{\Omega}\times\mathbf{u}))_i\right\}, \tag{1}$$

where subscript followed by "," comma denotes partial derivative w.r.t. space variable, and the superimposed dot denotes time derivative. $\boldsymbol{\Omega}\times(\boldsymbol{\Omega}\times\mathbf{u})$ represents the centripetal acceleration due to the time-varying motion and $2\boldsymbol{\Omega}\times\dot{\boldsymbol{u}}$ denotes Coriolis acceleration.

For very high magnetic field strength, Hall current term is also introduced, so generalized Ohm's law (Othman and Abd-Elaziz 2019) is written as

$$J_{\boldsymbol{i}} + \omega_e t_e \varepsilon_{ilk} J_l H_k = \sigma_0\left(E_i + \mu_0\varepsilon_{ijr}\dot{u}_j H_r\right), \tag{2}$$

Equation (2) can also be written as

$$J = \frac{\sigma_0}{1+m^2}\left\{E + \mu_0(\dot{u}\times H) - \frac{\mu_0}{en_e}(J\times H)\right\}$$

Following Lotfy et al. (2020), the stress-displacement-strain-carrier density function relation is given by

$$\sigma_{ij} = \left(\lambda u_{r,r} - \beta T - \delta_n N\right)\delta_{ij} + \mu\left(u_{i,j}+u_{j,i}\right). \tag{3}$$

where, $T = \phi - a\phi_{,ij}$,
$\beta = (3\lambda + 2\mu)\alpha_T$,
$\delta_n = (3\lambda + 2\mu)d_n$,
Here, $a > 0$ is the two-temperature parameter.

For the semiconductors nanostructure medium, for the plasma transportation process, the equation of plasma diffusion is given by

$$\frac{\partial N(x,y,z,t)}{\partial t} = D_E\nabla^2 N(x,y,z,t) - \frac{N(x,y,z,t)}{\tau} + \kappa\frac{T}{\tau} \tag{4}$$

The fractional-order heat conduction equation with two temperatures (Kaur et al. 2020a, Mahdy et al. 2020) is given by

$$\begin{aligned} &K_{ij}\left(1+\frac{(\tau_T)^\alpha}{\alpha!}\frac{\partial^\alpha}{\partial t^\alpha}\right)\dot{\phi}_{,ji} + K^*_{ij}\left(1+\frac{(\tau_v)^\alpha}{\alpha!}\frac{\partial^\alpha}{\partial t^\alpha}\right)\phi_{,ji} - \frac{E_g}{\tau}\frac{\partial N(r,t)}{\partial t} \\ &= \left(1+\frac{(\tau_q)^\alpha}{\alpha!}\frac{\partial^\alpha}{\partial t^\alpha}+\frac{(\tau_q)^{2\alpha}}{2\alpha!}\frac{\partial^{2\alpha}}{\partial t^{2\alpha}}\right) \times\left[\rho C_E\ddot{T} + \beta_{ij}T_0\ddot{e}_{ij} - \rho\dot{Q}\right], \end{aligned} \tag{5}$$

where

$$\begin{cases} 0<\alpha<1 \text{ for weak conductivity,} \\ \alpha = 1 \text{ for normal conductivity,} \\ 1<\alpha\le 2 \text{ for strong conductivity,} \end{cases}$$

$K_{ij} = K_i\delta_{ij}, K^*_{ij} = K^*_i\delta_{ij},\ \ i$ is not summed.

Method and solution of the problem

Consider a nonlocal semiconducting magneto-thermoelastic homogeneous isotropic medium initially at a constant temperature T_0 and rotating about the y-axis with an angular velocity $\boldsymbol{\Omega} = (0, \Omega, 0)$. Consider orthogonal Cartesian coordinates (x, y, z) with origin on the surface $(z = 0)$ and the z-axis directing downwards in the semiconductor medium. For the 2-D dynamic problem in xz–plane, we consider displacement vector as

$$\boldsymbol{u} = (u, 0, w)(x, z, t). \tag{6}$$

Consider that a very high-intensity magnetic field $\boldsymbol{H_0} = (0, H_0, 0)$ is applied in the positive y-direction and also assuming that induced electric field $E = 0$, therefore from ohms law we have

$$J_y = 0. \tag{7}$$

and J_x and J_z are given as

$$J_x = \frac{\sigma_0\mu_0H_0}{1+m^2}\left(m\frac{\partial u}{\partial t} - \frac{\partial w}{\partial t}\right), \tag{8}$$

$$J_z = \frac{\sigma_0\mu_0H_0}{1+m^2}\left(\frac{\partial u}{\partial t} + m\frac{\partial w}{\partial t}\right). \tag{9}$$

Using Eqs. (6), (7), (8), (9) in Eqs. (1), (4), and (5), the equations for nonlocal 2-D semiconducting medium with 2T in the absence of heat source, i.e., taking $Q = 0$, are:

$$(\lambda+2\mu)\frac{\partial^2 u}{\partial x^2}+(\lambda+\mu)\frac{\partial^2 w}{\partial x\partial z}+\mu\frac{\partial^2 u}{\partial z^2}-\beta\frac{\partial}{\partial x}\left\{\phi-a\left(\frac{\partial^2\phi}{\partial x^2}+\frac{\partial^2\phi}{\partial z^2}\right)\right\}-\delta_n\frac{\partial N}{\partial x}-\left(1-\epsilon^2\left(\frac{\partial^2}{\partial x^2}+\frac{\partial^2}{\partial z^2}\right)\right)\frac{\sigma_0\mu_0^2H_0^2}{1+\ m^2}\left(\frac{\partial u}{\partial t}+m\frac{\partial w}{\partial t}\right)=\rho\left(1-\epsilon^2\left(\frac{\partial^2}{\partial x^2}+\frac{\partial^2}{\partial z^2}\right)\right)\left(\frac{\partial^2 u}{\partial t^2}-\Omega^2u+2\Omega\frac{\partial w}{\partial t}\right), \tag{10}$$

$$(\lambda+\mu)\frac{\partial^2 u}{\partial x\partial z}+\mu\frac{\partial^2 w}{\partial x^2}+(\lambda+2\mu)\frac{\partial^2 w}{\partial z^2}-\beta\frac{\partial}{\partial z}\left\{\phi-a\left(\frac{\partial^2\phi}{\partial x^2}+\frac{\partial^2\phi}{\partial z^2}\right)\right\}-\delta_n\frac{\partial N}{\partial z}+\left(1-\epsilon^2\left(\frac{\partial^2}{\partial x^2}+\frac{\partial^2}{\partial z^2}\right)\right)\frac{\sigma_0\mu_0^2H_0^2}{1+\ m^2}\left(m\frac{\partial u}{\partial t}-\frac{\partial w}{\partial t}\right)=\rho\left(1-\epsilon^2\left(\frac{\partial^2}{\partial x^2}+\frac{\partial^2}{\partial z^2}\right)\right)\times\left(\frac{\partial^2 w}{\partial t^2}-\Omega^2w-2\Omega\frac{\partial u}{\partial t}\right), \tag{11}$$

$$\frac{\partial N}{\partial t}=D_E\left(\frac{\partial^2 N}{\partial x^2}+\frac{\partial^2 N}{\partial z^2}\right)-\frac{N}{\tau}+\kappa\frac{T}{\tau}, \tag{12}$$

$$K\left(1+\frac{(\tau_t)^\alpha}{\alpha!}\frac{\partial^\alpha}{\partial t^\alpha}\right)\frac{\partial}{\partial t}\left(\frac{\partial^2\phi}{\partial x^2}+\frac{\partial^2\phi}{\partial z^2}\right)+K^*\left(1+\frac{(\tau_v)^\alpha}{\alpha!}\frac{\partial^\alpha}{\partial t^\alpha}\right)\left(\frac{\partial^2\phi}{\partial x^2}+\frac{\partial^2\phi}{\partial z^2}\right)-\frac{E_g}{\tau}\frac{\partial N}{\partial t}=\left(1+\frac{(\tau_q)^\alpha}{\alpha!}\frac{\partial^\alpha}{\partial t^\alpha}+\frac{(\tau_q)^{2\alpha}}{2\alpha!}\frac{\partial^{2\alpha}}{\partial t^{2\alpha}}\right)\left[\rho C_E\frac{\partial^2}{\partial t^2}\left[\phi-a\frac{\partial^2\phi}{\partial x^2}-a\frac{\partial^2\phi}{\partial z^2}\right]+\beta T_0\frac{\partial^2}{\partial t^2}\left\{\frac{\partial u}{\partial x}+\frac{\partial w}{\partial z}\right\}\right], \tag{13}$$

and the stress-displacement-carrier density function relation (3) can be written as

$$\sigma_{xx}=(\lambda+2\mu)\frac{\partial u}{\partial x}+\lambda\ \frac{\partial w}{\partial z}-\beta T-\delta_n N, \tag{14}$$

$$\sigma_{zz}=\lambda\frac{\partial u}{\partial x}+(\lambda+2\mu)\ \frac{\partial w}{\partial z}-\beta T-\delta_n N, \tag{15}$$

$$\sigma_{xz}=\mu\left(\frac{\partial u}{\partial z}+\frac{\partial w}{\partial x}\right). \tag{16}$$

The dimensionless quantities are assumed as:

$$\left(x',z',u',w',\epsilon'\right)=\frac{\omega^*}{c_1}(x,z,u,w,\epsilon);\ T'=\frac{\beta T}{\lambda+2\mu};\ \Omega'=\frac{1}{\omega^*}\Omega;\ \left(\sigma'_{xx},\sigma'_{xz},\sigma'_{zz}\right)=\frac{1}{\lambda+2\mu}(\sigma_{xx},\sigma_{xz},\sigma_{zz});\ a'=\left(\frac{\omega^*}{c_1}\right)^2,\ \left(\tau'_T,\tau'_v,\tau'_q,t'\right)=\omega^*\left(\tau_T,\tau_v,\tau_q,t\right),\ \phi'=\frac{\beta\phi}{\lambda+2\mu},\ \left(\phi',\psi'\right)=\left(\frac{\omega^*}{c_1}\right)^2(\phi,\psi),\ N'=\frac{\delta_n N}{\lambda+2\mu},\ \omega^*=\frac{\rho C_E c_1^2}{K},\ c_1^2=\frac{\lambda+2\mu}{\rho},\ c_2^2=\frac{\mu}{\rho},\ \delta^2=\frac{c_2^2}{c_1^2},\ M=\frac{\sigma_0\mu_0^2H_0^2}{\rho\omega^*}. \tag{17}$$

Using (17) in Eqs. (10), (11), (12), (13) and after suppressing the primes yields

$$\frac{\partial^2 u}{\partial x^2}+\left(1-\delta^2\right)\frac{\partial^2 w}{\partial x\partial z}+\delta^2\frac{\partial^2 u}{\partial z^2}-\frac{\partial}{\partial x}\left\{\phi-a\left(\frac{\partial^2\phi}{\partial x^2}+\frac{\partial^2\phi}{\partial z^2}\right)\right\}-\frac{\partial N}{\partial x}=\left(1-\epsilon^2\left(\frac{\partial^2}{\partial x^2}+\frac{\partial^2}{\partial z^2}\right)\right)\left\{\frac{M}{1+m^2}\left[\frac{\partial u}{\partial t}+m\frac{\partial w}{\partial t}\right]+\left(\frac{\partial^2 u}{\partial t^2}-\Omega^2u+2\Omega\frac{\partial w}{\partial t}\right)\right\}, \tag{18}$$

$$\left(1-\delta^2\right)\frac{\partial^2 u}{\partial x\partial z}+\delta^2\frac{\partial^2 w}{\partial x^2}+\frac{\partial^2 w}{\partial z^2}-\frac{\partial}{\partial z}\left\{\phi-a\left(\frac{\partial^2\phi}{\partial x^2}+\frac{\partial^2\phi}{\partial z^2}\right)\right\}-\frac{\partial N}{\partial z}=\left(1-\epsilon^2\left(\frac{\partial^2}{\partial x^2}+\frac{\partial^2}{\partial z^2}\right)\right)\left\{\frac{-M}{1+m^2}\left[m\frac{\partial u}{\partial t}-\frac{\partial w}{\partial t}\right]+\left(\frac{\partial^2 w}{\partial t^2}-\Omega^2w-2\Omega\frac{\partial u}{\partial t}\right)\right\}, \tag{19}$$

$$\left[\left(\frac{\partial^2}{\partial x^2}+\frac{\partial^2}{\partial z^2}\right)-\delta_1\left(\frac{\partial}{\partial t}+\delta_2\right)\right]N + \varepsilon_3\left\{\phi-a\left(\frac{\partial^2\phi}{\partial x^2}+\frac{\partial^2\phi}{\partial z^2}\right)\right\} = 0, \tag{20}$$

$$\left(1+\frac{(\tau_t)^\alpha}{\alpha!}\frac{\partial^\alpha}{\partial t^\alpha}\right)\frac{\partial}{\partial t}\left(\frac{\partial^2\phi}{\partial x^2}+\frac{\partial^2\phi}{\partial z^2}\right) + \frac{K^*}{K\omega^*}\left(1+\frac{(\tau_v)^\alpha}{\alpha!}\frac{\partial^\alpha}{\partial t^\alpha}\right)\left(\frac{\partial^2\phi}{\partial x^2}+\frac{\partial^2\phi}{\partial z^2}\right) + \varepsilon_2\frac{\partial N}{\partial t} = \left(1+\frac{(\tau_q)^\alpha}{\alpha!}\frac{\partial^\alpha}{\partial t^\alpha}+\frac{(\tau_q)^{2\alpha}}{2\alpha!}\frac{\partial^{2\alpha}}{\partial t^{2\alpha}}\right) \times\left[\frac{\partial^2}{\partial t^2}\left\{\phi-a\left(\frac{\partial^2\phi}{\partial x^2}+\frac{\partial^2\phi}{\partial z^2}\right)\right\}+\varepsilon_1\left\{\frac{\partial\ddot{u}}{\partial x}+\frac{\partial\ddot{w}}{\partial z}\right\}\right], \tag{21}$$

where

$$\delta_1=\frac{c_1^2}{D_E\omega^*},\ \varepsilon_3=\frac{\kappa K d_n}{\alpha_T\rho C_E D_E\omega^*\tau'},\ \varepsilon_2 = \frac{E_g\alpha_T}{d_n\rho C_E(\omega^*)^2\tau'},\ \varepsilon_1=\frac{\beta^2T_0}{\rho C_E(\lambda+2\mu)},\ \delta_2=\frac{1}{\tau},$$

The parameter ε_1 is thermoelastic coupling parameter as it depends on thermoelastic properties (i.e., specific heat, Lame's elastic constants, and temperature T_0). The parameter ε_3 is thermoelectric coupling parameter as it depends on thermoelectrical properties (i.e., coefficient of electronic deformation d_n).

By using Eq. (17) in Eqs. (14), (15), (16) and after suppressing the primes, it yields

$$\sigma_{xx}(x,z,t)=\frac{\partial u}{\partial x} + \left(1-2\delta^2\right)\frac{\partial w}{\partial z}-\left\{\phi-a\left(\frac{\partial^2\phi}{\partial x^2}+\frac{\partial^2\phi}{\partial z^2}\right)\right\}-N, \tag{22}$$

$$\sigma_{zz}(x,z,t)=\left(1-2\delta^2\right)\frac{\partial u}{\partial x} + \frac{\partial w}{\partial z}-\left\{\phi-a\left(\frac{\partial^2\phi}{\partial x^2}+\frac{\partial^2\phi}{\partial z^2}\right)\right\}-N, \tag{23}$$

$$\sigma_{xz}(x,z,t)=\delta^2\left(\frac{\partial u}{\partial z}+\frac{\partial w}{\partial x}\right), \tag{24}$$

We now present the potential functions ϕ and ψ as

$$u=\frac{\partial\phi}{\partial x}-\frac{\partial\psi}{\partial z},\ w=\frac{\partial\phi}{\partial z}+\frac{\partial\psi}{\partial x},\ e=\nabla^2\phi,\ \frac{\partial w}{\partial x}-\frac{\partial u}{\partial z} = \nabla^2\psi, \tag{25}$$

Using (25) in Eqs. (18), (19), (20), (21) yields

$$\delta^2\nabla^2\psi+\left\{\phi-a\nabla^2\phi\right\}+N = \left(1-\epsilon^2\nabla^2\right) \left\{\frac{M}{1+m^2}\left[\frac{\partial\psi}{\partial t}-m\frac{\partial\phi}{\partial t}\right]+\left(\frac{\partial^2\psi}{\partial t^2}-\Omega^2\psi-2\Omega\frac{\partial\phi}{\partial t}\right)\right\}, \tag{26}$$

$$\nabla^2\phi=\left(1-\epsilon^2\nabla^2\right) \left\{\frac{M}{1+m^2}\left[m\frac{\partial\psi}{\partial t}+\frac{\partial\phi}{\partial t}\right]+\left(\frac{\partial^2\phi}{\partial t^2}-\Omega^2\phi+2\Omega\frac{\partial\psi}{\partial t}\right)\right\}, \tag{27}$$

$$\left[\nabla^2-\delta_1\left(\frac{\partial}{\partial t}+\delta_2\right)\right]N+\varepsilon_3\left\{\phi-a\nabla^2\phi\right\}=0 \tag{28}$$

$$\left\{\left(1+\frac{(\tau_t)^\alpha}{\alpha!}\frac{\partial^\alpha}{\partial t^\alpha}\right)\frac{\partial}{\partial t}+\frac{K^*}{K\omega^*}\left(1+\frac{(\tau_v)^\alpha}{\alpha!}\frac{\partial^\alpha}{\partial t^\alpha}\right)\right\}\nabla^2\phi + \varepsilon_2\frac{\partial N}{\partial t} = \left(1+\frac{(\tau_q)^\alpha}{\alpha!}\frac{\partial^\alpha}{\partial t^\alpha}+\frac{(\tau_q)^{2\alpha}}{2\alpha!}\frac{\partial^{2\alpha}}{\partial t^{2\alpha}}\right) \times\left[\frac{\partial^2}{\partial t^2}\left\{\phi-a\nabla^2\phi\right\}+\varepsilon_1\frac{\partial^2}{\partial t^2}\nabla^2\phi\right], \tag{29}$$

where

$$\nabla^2\equiv\frac{\partial^2}{\partial x^2}+\frac{\partial^2}{\partial z^2}.$$

The stress displacement carrier density relations becomes

$$\sigma_{xx}(x,z,t)=\left(\frac{\partial^2\phi}{\partial x^2}-\frac{\partial^2\psi}{\partial x\partial z}\right) + \left(1-2\delta^2\right) \left(\frac{\partial^2\phi}{\partial z^2}+\frac{\partial^2\psi}{\partial x\partial z}\right)-\left\{\phi-a\left(\frac{\partial^2\phi}{\partial x^2}+\frac{\partial^2\phi}{\partial z^2}\right)\right\}-N, \tag{30}$$

$$\sigma_{zz}(x,z,t)=\left(1-2\delta^2\right) \times\left(\frac{\partial^2\phi}{\partial x^2}-\frac{\partial^2\psi}{\partial x\partial z}\right) + \left(\frac{\partial^2\phi}{\partial z^2}+\frac{\partial^2\psi}{\partial x\partial z}\right)-\left\{\phi-a\left(\frac{\partial^2\phi}{\partial x^2}+\frac{\partial^2\phi}{\partial z^2}\right)\right\}-N, \tag{31}$$

$$\sigma_{xz}(x,z,t)=\delta^2\left(2\frac{\partial^2\phi}{\partial x\partial z}-\frac{\partial^2\psi}{\partial z^2}+\frac{\partial^2\psi}{\partial x^2}\right), \tag{32}$$

Plane-wave propagation

Consider the plane wave solution of the Eqs. (26), (27), (28), (29) of the form

$$\begin{pmatrix} \phi \\ \psi \\ \varphi \\ N \end{pmatrix} = \begin{pmatrix} \overline{\phi} \\ \overline{\psi} \\ \overline{\varphi} \\ \overline{N} \end{pmatrix} e^{(i\xi(x\ sin\theta + z\ cos\theta) - i\omega t)}, \tag{33}$$

where $sin\theta,\ cos\theta$ indicates the projection of wave normal to the $x-z$ plane, ω represents angular frequency and ξ denotes the wavenumber of a plane wave propagating in $x-z$ plane and $\overline{\phi}, \overline{\psi}, \overline{\varphi}, \overline{N}$ are the constants to be determined .

Using Eq. (33) in Eqs. (26), (27), (28), (29) yields

$$\left[\zeta_2 + \zeta_4\xi^2\right]\overline{\phi} + \left[\zeta_1 + \zeta_3\xi^2\right]\overline{\psi} + \left[1 + a\xi^2\right]\overline{\varphi} + \overline{N} = 0, \tag{34}$$

$$\left[\zeta_6\xi^2 + \zeta_5\right]\overline{\phi} + \left[\zeta_8\xi^2 + \zeta_7\right]\overline{\psi} - = 0, \tag{35}$$

$$\varepsilon_3\left[1 + a\xi^2\right]\overline{\varphi} + \left[\zeta_9 - \xi^2\right]\overline{N} = 0, \tag{36}$$

$$\zeta_{13}\xi^2\overline{\phi} + \left[\zeta_{12}\xi^2 + \zeta_{10}\right]\overline{\varphi} + \varepsilon_2 i\omega\overline{N} = 0. \tag{37}$$

And the stress-strain relations can be written as

$$\sigma_{xx} = \left[-\xi^2\left(sin^2\theta + \left(1-2\delta^2\right) cos^2\theta\right)\overline{\phi} + \xi^2\left(-2\delta^2\right)\frac{\sin 2\theta}{2}\overline{\psi} - \left[1 + a\xi^2\right]\overline{\varphi} - \overline{N}\right] e^{(i\xi(x\ sin\theta + z\ cos\theta) - i\omega t)} \tag{38}$$

$$\sigma_{zz} = \left[-\xi^2\left(\left(1-2\delta^2\right) sin^2\theta + cos^2\theta\right)\overline{\phi} + \xi^2\left(-2\delta^2\right)\frac{\sin 2\theta}{2}\overline{\psi} - \left[1 + a\xi^2\right]\overline{\varphi} - \overline{N}\right] e^{(i\xi(x\ sin\theta + z\ cos\theta) - i\omega t)}, \tag{39}$$

$$\sigma_{xz}(x, z, t) = -\xi^2\delta^2\left(\sin 2\theta\overline{\phi} + \cos 2\theta\overline{\psi}\right) e^{(i\xi(x\ sin\theta + z\ cos\theta) - i\omega t)}, \tag{40}$$

Where, $\zeta_1 = \left(\frac{i\omega M}{1+m^2} + \omega^2 + \Omega^2\right)$,

$$\zeta_2 = -\left(\frac{Mmi\omega}{1 + m^2} + 2\omega\Omega i\right),$$

$$\zeta_3 = \zeta_1\epsilon^2 - \delta^2,$$

$$\zeta_4 = \zeta_2\epsilon^2,$$

$$\zeta_5 = \frac{Mi\omega}{1 + m^2} + \omega^2 + \Omega^2,$$

$$\zeta_6 = \zeta_5\epsilon^2 - 1,$$

$$\zeta_7 = \frac{Mmi\omega}{1 + m^2} + 2\omega\Omega i,$$

$$\zeta_8 = \zeta_7\epsilon^2,$$

$$\zeta_9 = \delta_1(i\omega - \delta_2),$$

$$\zeta_{10} = \left[1 + \frac{\tau_q^\alpha}{\alpha!}(-i\omega)^\alpha + \frac{\tau_q^{2\alpha}}{2\alpha!}(-i\omega)^{2\alpha}\right]\omega^2,$$

$$\zeta_{11} = \left[1 + \frac{\tau_T^\alpha}{\alpha!}(-i\omega)^\alpha\right] i\omega - \frac{K^*}{K\omega^*}\left[1 + \frac{\tau_\nu^\alpha}{\alpha!}(-i\omega)^\alpha\right],$$

$$\zeta_{13} = -\zeta_{10}\varepsilon_1,$$

$$\zeta_{12} = (\zeta_{11} - \zeta_{10}a).$$

Eliminating $\overline{\phi}, \overline{\psi}, \overline{\varphi}$ and $\overline{N}$ from the Eqs. (34), (35), (36), (37) yields the characteristic equation as

$$A\xi^8 + B\xi^6 + C\xi^4 + D\xi^2 + E = 0, \tag{41}$$

where

$A = -\zeta_{13}\zeta_9\zeta_8 a + \zeta_{12}\zeta_4\zeta_8 - \zeta_3\zeta_6\zeta_{12}$,

$B = -a\varepsilon_3\zeta_{13}\zeta_8 + \varepsilon_2 i\omega\varepsilon_3\zeta_4\zeta_8 a - a\varepsilon_2 i\omega\varepsilon_3\zeta_6\zeta_3 - \zeta_{13}\zeta_9\zeta_7 a + \zeta_{13}\zeta_9\zeta_8 a - \zeta_{13}\zeta_9\zeta_8 a + \zeta_{12}\zeta_2\zeta_8 - \zeta_1\zeta_6\zeta_{12} - \zeta_{12}\zeta_9\zeta_4\zeta_8 + \zeta_{10}\zeta_4\zeta_8 + \zeta_{12}\zeta_9\zeta_6\zeta_3 - \zeta_3\zeta_6\zeta_{10} + \zeta_{12}\zeta_4\zeta_7 - \zeta_{12}\zeta_5\zeta_3$,

$C = \zeta_{13}\zeta_9\zeta_8 + \zeta_{13}\zeta_9\zeta_7 a - \zeta_{13}\zeta_9\zeta_7 - \varepsilon_3\zeta_{13}\zeta_8 - \varepsilon_3\zeta_{13}\zeta_7 + (\varepsilon_2\varepsilon_3\zeta_4\zeta_8 - \varepsilon_2\varepsilon_3\zeta_6\zeta_3)i\omega + (\varepsilon_2\varepsilon_3\zeta_2\zeta_8 + \varepsilon_2\varepsilon_3\zeta_4\zeta_7 - \varepsilon_2\varepsilon_3\zeta_6\zeta_1 - \varepsilon_2\varepsilon_3\zeta_5\zeta_3)ai\omega - \zeta_{12}\zeta_9\zeta_2\zeta_8 + \zeta_{10}\zeta_2\zeta_8 + \zeta_{12}\zeta_6\zeta_1\zeta_9 - \zeta_{10}\zeta_1\zeta_6 - \zeta_{10}\zeta_9\zeta_4\zeta_8 - \zeta_{12}\zeta_5\zeta_1 + \zeta_{12}\zeta_2\zeta_7 - \zeta_{12}\zeta_4\zeta_7\zeta_9 + \zeta_{10}\zeta_4\zeta_7 + \zeta_{12}\zeta_9\zeta_5\zeta_3 - \zeta_{10}\zeta_5\zeta_3$,

$$\begin{aligned} D = {} & \zeta_{13}\zeta_9\zeta_7 - \varepsilon_3\zeta_{13}\zeta_7 + i\omega(\varepsilon_2\varepsilon_3\zeta_2\zeta_8 \\ & + \varepsilon_2\varepsilon_3\zeta_4\zeta_7 - \varepsilon_2\varepsilon_3\zeta_6\zeta_1 - \varepsilon_2\varepsilon_3\zeta_5\zeta_3 \\ & + a\varepsilon_2\varepsilon_3\zeta_2\zeta_7 - a\varepsilon_2\varepsilon_3\zeta_5\zeta_1) - \zeta_{10}\zeta_9\zeta_2\zeta_8 + \zeta_{10}\zeta_9\zeta_1\zeta_6 \\ & + \zeta_{12}\zeta_9\zeta_5\zeta_1 - \zeta_{10}\zeta_1\zeta_5 + \zeta_{10}\zeta_7\zeta_2 - \zeta_{10}\zeta_9\zeta_4\zeta_7 + \zeta_{10}\zeta_9\zeta_3\zeta_5 \end{aligned}$$

$E = i\omega(\varepsilon_2\varepsilon_3\zeta_2\zeta_7 - \varepsilon_2\varepsilon_3\zeta_5\zeta_1) + \zeta_{10}\zeta_9\zeta_5\zeta_1 - \zeta_{12}\zeta_9\zeta_2\zeta_7 - \zeta_{10}\zeta_9\zeta_2\zeta_7 + \zeta_{10}\zeta_9\zeta_3\zeta_6$.

The solution of Eq. (41) give eight roots in ξ that is, $\pm\xi_1, \pm\xi_2, \pm\xi_3, \pm\xi_4$, and we are concerned with the positive imaginary parts of the roots. When a coupled longitudinal wave falls on the boundary $z = 0$, four reflected waves are generated. It exhibits that the generated waves are coupled in nature. Corresponding to positive four roots and descending order of their velocities, four coupled waves are transmitted, specifically CLD wave related with ϕ transmitting with the maximum speed V_1, CT-wave linked with the φ having speed V_2 and CCD-wave related with N having speed V_3 and CTD-wave linked with the vector potential ψ transmitting with the lowest speed V_4. Following Lata et al. (2021), the characteristics properties of these waves are obtained by the following expressions

(i) Phase velocity

The phase velocities of the plane wave is represented as

$$V_j = \frac{\omega}{Re(\xi_j)}, \mathrm{j} = 1, 2, 3, 4$$

(ii) Attenuation coefficient

The attenuation coefficient of the plane wave is represented as

$$Q_j = Img(\xi_j), \mathrm{j} = 1, 2, 3, 4.$$

(iii) Specific loss

The specific loss of the plane wave is represented as:

$$W_j = \left(\frac{\Delta W}{W}\right)_j = 4\pi\left|\frac{Img(\xi_j)}{Re(\xi_j)}\right|, \mathrm{j} = 1, 2, 3, 4.$$

ΔW is the energy dissipated and W is the energy stored.

(iv) Penetration depth

The penetration depth is given by

$$S_j = \frac{1}{Img(\xi_j)}, \mathrm{j} = 1, 2, 3, 4.$$

Particular cases

1. For nonlocal semiconductor medium with rotation, Hall current, and two temperatures ($m, a, \alpha, \Omega, \xi$) > 0, from the above relations, the following cases can also be obtained
   i. Three-phase lag FOT (TPL-FOT)
   If $\tau_q > \tau_T > \tau_\nu \geq 0$.
   ii. Dual-phase lag FOT (DPL-FOT)
   If $\tau_\nu = 0, K^*_{ij} = 0 \ \ \tau_q > \tau_T \geq 0$.
   iii. Single-phase lag FOT (SPL-FOT) or Lord–Shulman MDD
   If $\tau_T = 0,\ \tau_\nu = 0,\ \tau_q = \tau_0 > 0$ and $K^*_{ij} = 0$, and ignoring τ_q^2.
   iv. Three-phase lag (TPL)
   If $\tau_q > \tau_T > \tau_\nu \geq 0, \alpha = 1, G_{\tau_q} = G_{\tau_\nu} = G_{\tau_T} = i\omega$
   v. Dual-phase lag (DPL)
   If $\tau_\nu = 0, K^*_{ij} = 0 \ \ \alpha = 1$,and $\tau_q > \tau_T \geq 0, G_{\tau_q} = G_{\tau_T} = i\omega$
   vi. Single-phase lag (SPL) or Lord–Shulman model
   If $\tau_T = 0,\ \tau_\nu = 0,\ \tau_q = \tau_0 > 0 \ \ \alpha = 1$,and $K^*_{ij} = 0$, and ignoring τ_q^2. $G_{\tau_q} = i\omega$
   vii. GN theory of Type-III
   If $\tau_T = 0,\ \tau_\nu = 0,\ \tau_q = 0 \ \ \alpha = 1$,and $K^*_{ij} \neq 0, K_{ij} \neq 0$
   viii. GN theory of Type-II
   If $\tau_T = 0,\ \tau_\nu = 0,\ \tau_q = 0 \ \ \alpha = 1$, and $K_{ij} = 0$
   ix. GN theory of Type-I
   If $\tau_T = 0,\ \tau_\nu = 0,\ \tau_q = 0 \ \ K^*_{ij} = 0, \alpha = 1$.
2. For local semiconductor medium $\epsilon = 0$, for all the above $a - j$ cases
3. For semiconductor medium without rotation, $\Omega = 0$, for all the above $a - j$ cases
4. For semiconductor medium without Hall current m=0, for all the above $a - j$ cases
5. For semiconductor medium without two temperatures $a = 0$, for all the above $a - j$ cases
6. For semiconductor medium without FOT $\alpha = 0$, for all the above $a - j$ cases

Numerical results and discussion

To demonstrate the theoretical results and effect of Hall current, fractional order parameter, two temperatures, and non-local parameter, the physical data for semiconducting medium taken from Mahdy et al. (2020) is given as

$$\begin{aligned}\lambda &= 3.64 \times 10^{10}\ Nm^{-2}, \quad \mu = 5.46 \times 10^{10}\ Nm^{-2}, \quad \beta\\ &= 7.04 \times 10^{6} Nm^{-2}\ deg^{-1}, \quad d_n\\ &= -9 \times 10^{-31}\ m^{-3}, \quad \rho = 2.33 \times 10^{3} Kgm^{-3}, \quad C_E\\ &= 695\ JKg^{-1}K^{-1}, K = 150\ Wm^{-1}K^{-1}, K^*\\ &= 1.54 \times 10^{2}\, Ws, \quad \mathrm{T_0} = 800\ \mathrm{K}, \tau_T = 1 \times 10^{-7}\tau_\nu\\ &= 2 \times 10^{-8} s, \tau_q = 2 \times 10^{-7}\mathrm{s}, D_E\\ &= 2.5 \times 10^{-3}\ m^2 s^{-1}, \mathrm{H_0} = 1\ \mathrm{Jm^{-1}nb^{-1}}, \tau\\ &= 5 \times 10^{-5}\ \mathrm{s}, \quad N_0 = 10^{20} m^{-3}, s_0 = 2\ ms^{-1}, \varepsilon_0\\ &= 8.838 \times 10^{-12}\,\mathrm{Fm^{-1}}, E_g = 1.11 eV, \alpha_T\\ &= 3 \times 10^{-6} K^{-1}.\end{aligned}$$

Figures 1, 2, 3, and 4 indicate the change of phase velocities w.r.t. frequency ω respectively. Figure 1 illustrates the change in phase velocity with the change in fractional order heat transfer parameter α. Figure 2 illustrates the change in phase velocity with the change in Hall current parameter m. As the Hall current increases, phase velocity decreases. Figure 3 illustrates the change in phase velocity with the change in two-temperature parameter a. The higher the value of two temperatures, the lower is the phase velocity of the plane wave.

Figure 4 illustrates the change in phase velocity with the change in non-local parameter ϵ. The higher the value of ϵ, the lower is the phase velocity of plane wave.

Figures 5, 6, 7, and 8 indicate the change of attenuation coefficients w.r.t. frequency ω respectively. Figure 5 illustrates the change in attenuation coefficients with the change in fractional order heat transfer parameter α. For the initial value of the frequency, attenuation

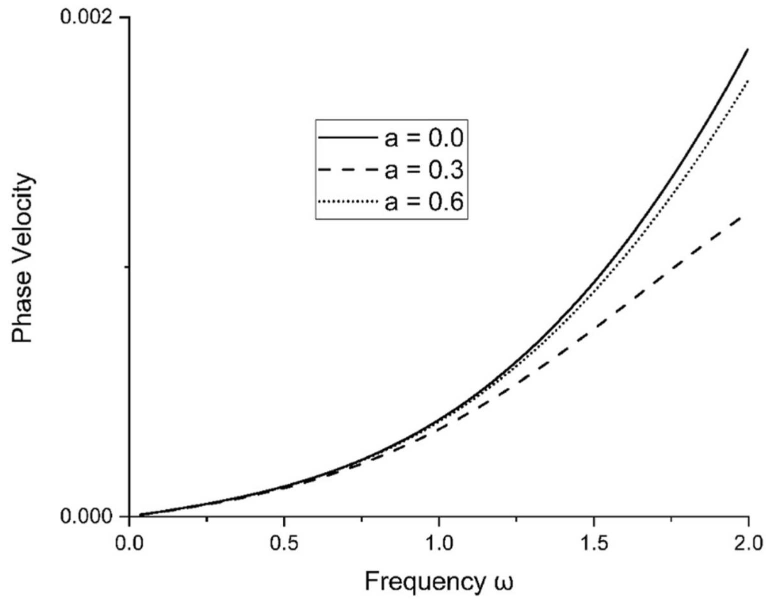

Fig. 1 Phase velocity w.r.t $\boldsymbol{\omega}$ and fractional order heat transfer parameter $\boldsymbol{\alpha}$

coefficients decrease sharply. The higher the value of α, the higher is the attenuation coefficients. Figure 6 illustrates the change in attenuation coefficients with the change in Hall current parameter m. For the initial value of the frequency, attenuation coefficients decrease sharply. However, As the Hall current increases, attenuation coefficients decrease. Figure 7 illustrates the change in attenuation coefficients with the change in two-temperature parameter a. The higher the value of two temperature, the lower is the attenuation coefficients of a plane wave. Figure 8 illustrates the change in attenuation coefficients with the change in non-local parameter ϵ . The higher the value of parameter ϵ, the lower is the attenuation coefficients of a plane wave.

Figures 9, 10, 11, and 12 indicate the change of specific loss w.r.t. frequency ω respectively. Figure 9 illustrates

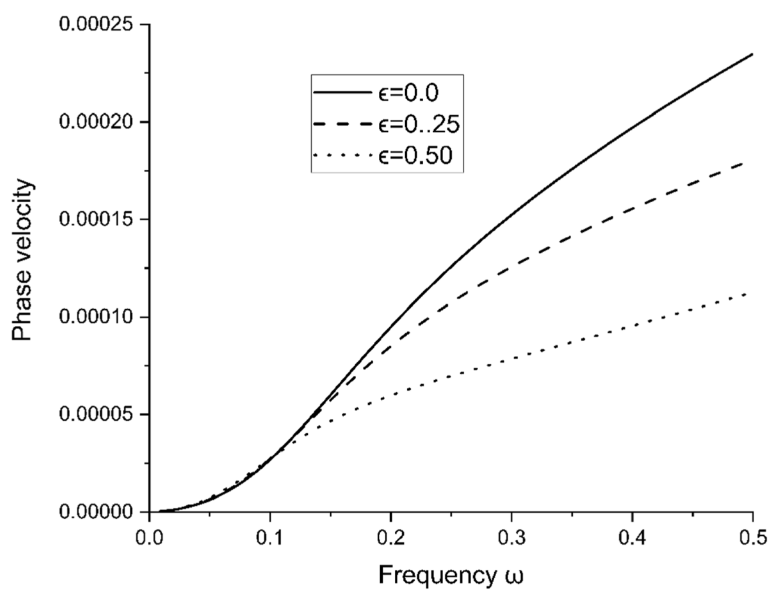

Fig. 2 Phase velocity w.r.t $\boldsymbol{\omega}$ and Hall current parameter $\boldsymbol{m}$

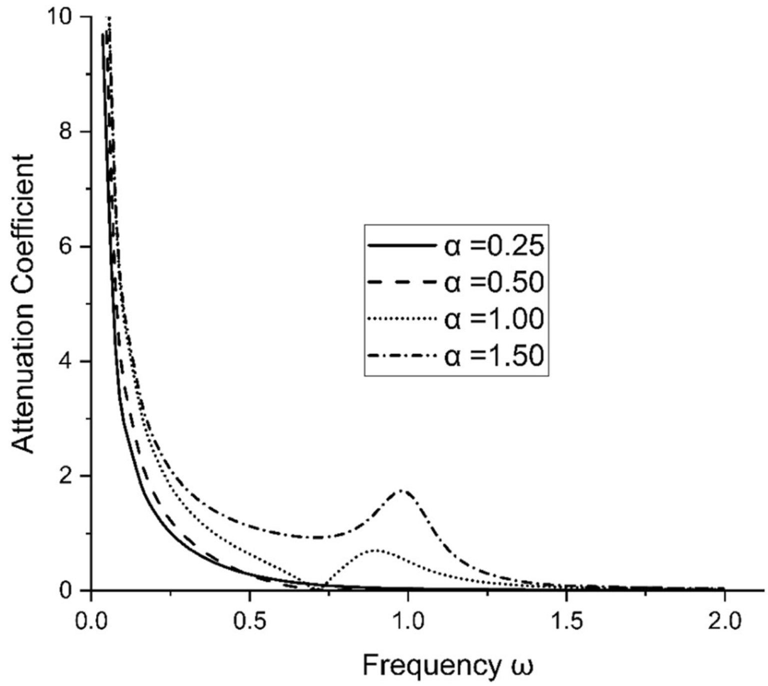

Fig. 3 Phase velocity w.r.t $\boldsymbol{\omega}$ and two-temperature parameter $\boldsymbol{a}$

the change in specific loss with the change in fractional order heat transfer parameter α. The higher the value of α, the higher is the specific loss. Figure 10 illustrates the change in specific loss with the change in Hall current parameter m. As the Hall current increases, specific loss decreases. Figure 11 illustrates the change in specific loss with the change in two-temperature parameter a. The higher the value of two temperatures, the lower is the specific loss of plane wave. Figure 12 illustrates the change in specific loss with the change in non-local parameter ϵ. The higher the value of ϵ, the lower is the specific loss of plane wave.

Figures 13, 14, 15, and 16 indicate the change of penetration depth w.r.t. frequency ω respectively. Figure 13

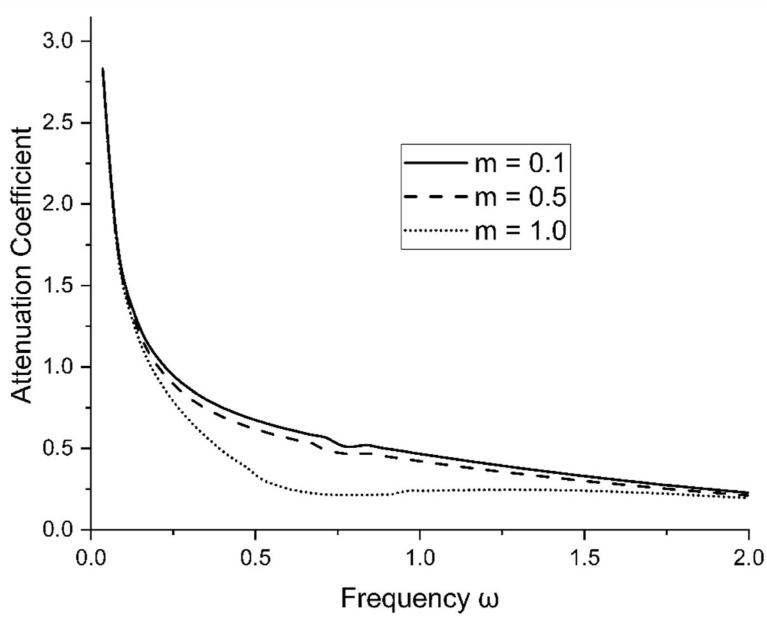

Fig. 4 Phase velocity w.r.t $\boldsymbol{\omega}$ and non-local parameter $\boldsymbol{\epsilon}$

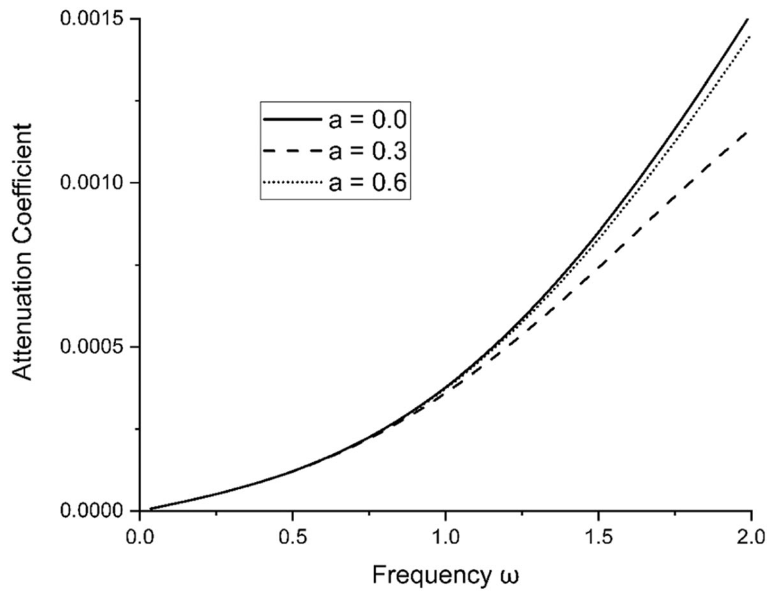

Fig. 5 Attenuation coefficient w.r.t ***ω*** and fractional order heat transfer parameter ***α***

illustrates the change in penetration depth with the change in fractional order heat transfer parameter α The higher the value of α, the higher is the penetration depth. Figure 14 illustrates the change in penetration depth with the change in Hall current parameter m. For the initial value of the frequency, penetration depth increases sharply, and after half range of frequency, it decreases. However, the higher the value of Hall current increases, the higher is the penetration depth. Figure 15 illustrates the change in penetration depth with the change in two temperature parameter a. The higher the value of two temperature, the lower is the penetration depth of plane wave. Figure 16 illustrates the change in penetration depth with the change in non-local

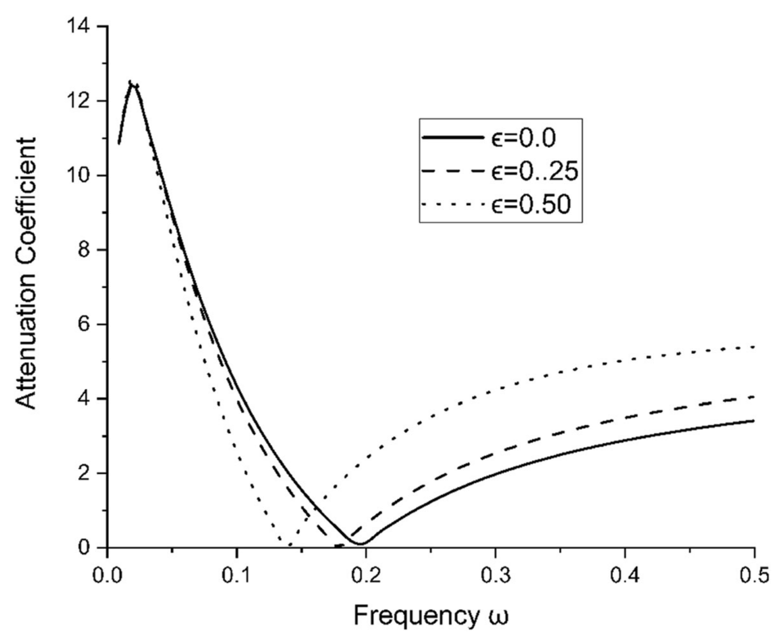

Fig. 6 Attenuation coefficient w.r.t ***ω*** and Hall current parameter ***m***

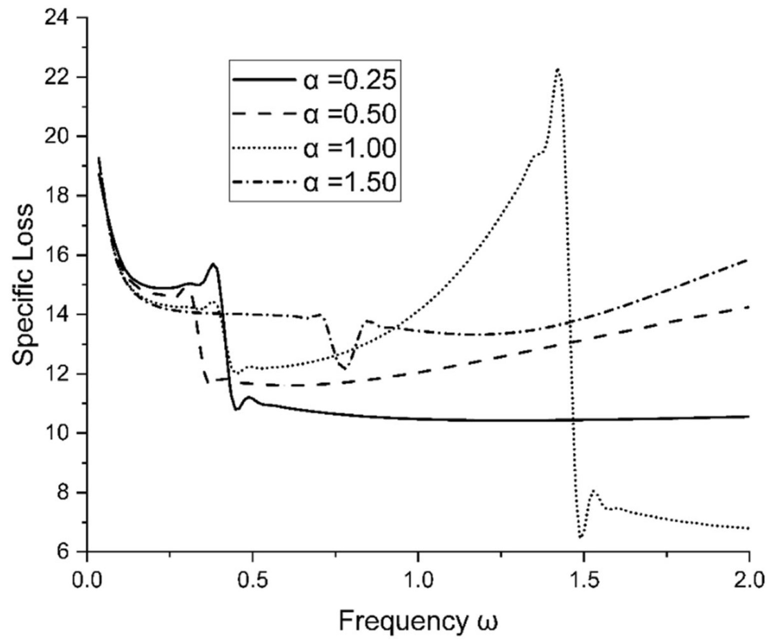

Fig. 7 Attenuation coefficient w.r.t ω and two temperature parameter a

parameter ϵ. The higher the value of non-local parameter ϵ, the lower is the penetration depth of plane wave.

Conclusions

- In this study, the propagation of plane harmonic waves in magneto-thermoelastic rotating semiconducting medium has been studied.
- The semiconducting medium is rotating with angular frequency Ω and is under the influence of high magnetic field. The governing equations are modeled using the Hall current effect and fractional order three phase lag heat transfer with two temperature.
- The non-dimensional expressions for penetration depth, phase velocities, specific loss, and attenuation coefficients of various reflected waves are calculated

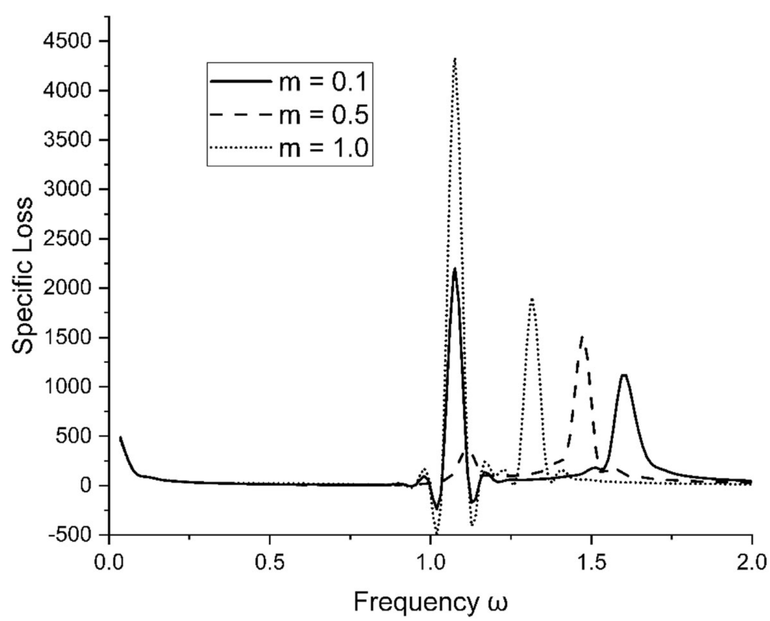

Fig. 8 Attenuation coefficient w.r.t ω and non-local parameter ϵ

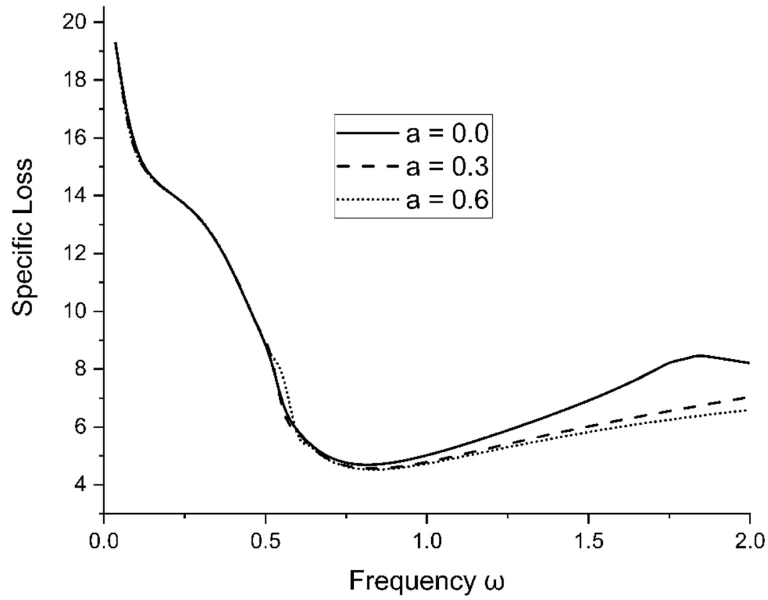

Fig. 9 Specific loss w.r.t ***ω*** and fractional order heat transfer parameter ***α***

and drawn graphically with the help of MATLAB software.

- Effect of fractional order heat transfer, Hall current, two-temperature, and non-local parameter ϵ on the penetration depth, phase velocities, specific loss, and attenuation coefficients of various reflected waves are represented graphically. The results exhibit that as the value of fractional order heat transfer parameter α increases, variations in the penetration depth, phase velocities, specific loss, and attenuation coefficients also increases. The higher the value of Hall current, the lower will be the penetration depth, phase velocities, specific loss, and attenuation coefficients of the plane wave. However, two-temperature parameters show different behavior with different characteristics of a plane wave.

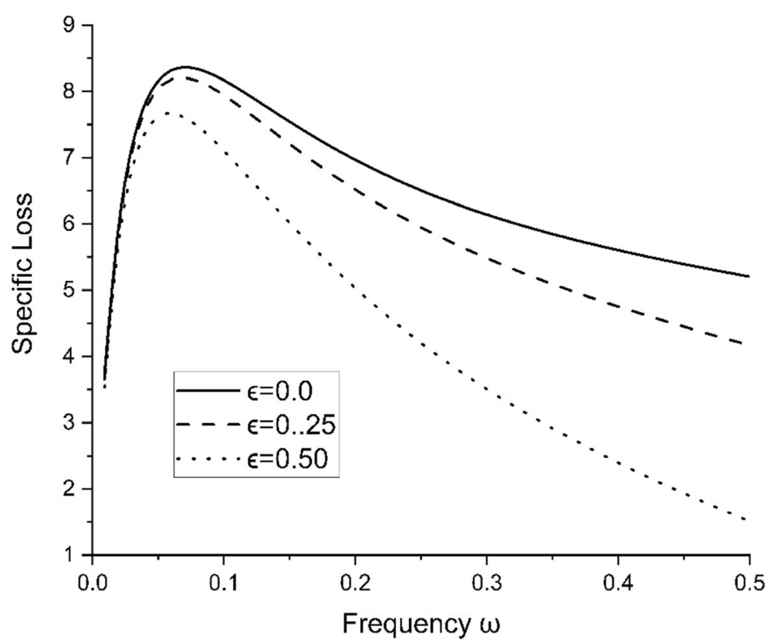

Fig. 10 Specific loss w.r.t ***ω*** and Hall current parameter ***m***

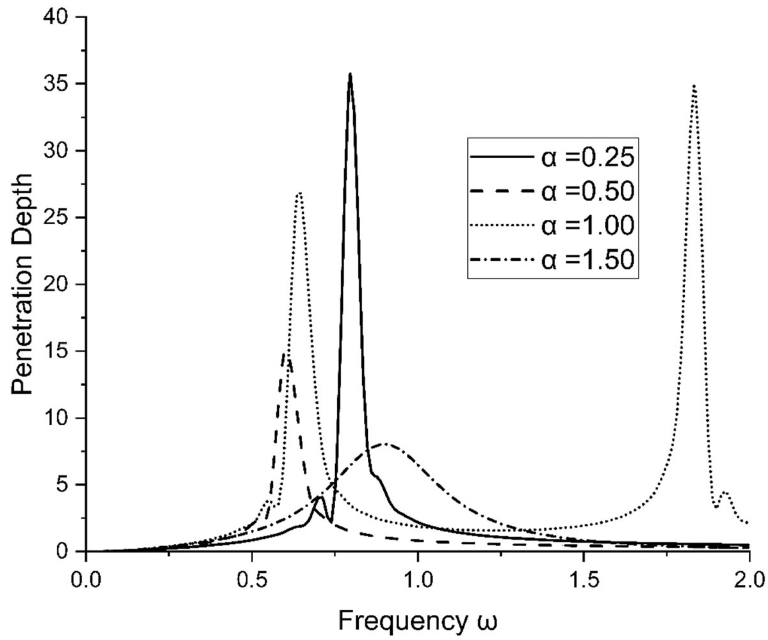

Fig. 11 Specific loss w.r.t $\boldsymbol{\omega}$ and two temperature parameter $\boldsymbol{a}$

- The non-local parameter ϵ has a significant effect on the penetration depth, phase velocities, specific loss, and attenuation coefficients of various reflected waves. The deviation in penetration depth, phase velocities, specific loss, and attenuation coefficients of various reflected waves is higher when $\epsilon = 0$, as the value of ϵ increases, the variations in penetration depth, phase velocities, specific loss, and attenuation coefficients of various reflected waves decrease.
- The study may help in the design of semiconductor nano-devices, Hall effect sensors, magnetic switches, applications in the automotive world, geology, and seismology as well as semiconductor nanostructure devices such as MEMS/NEMS.

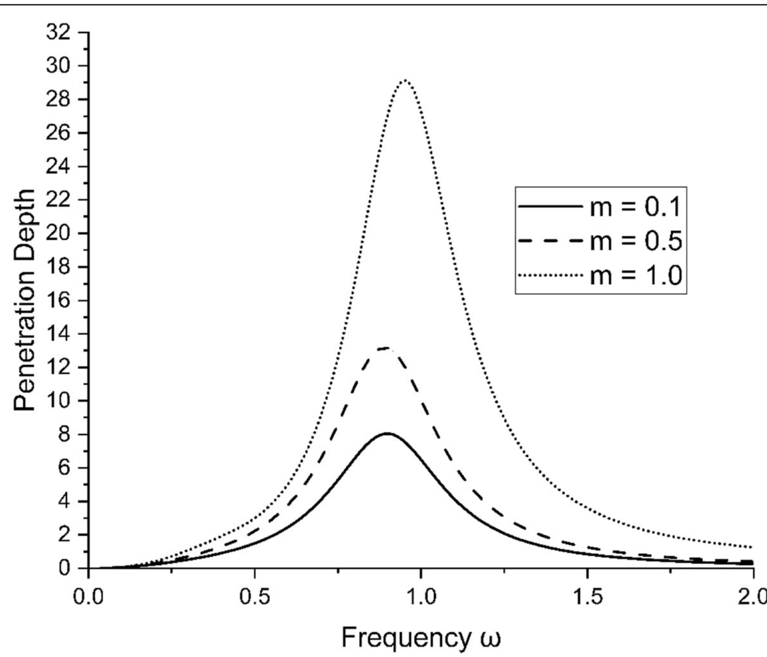

Fig. 12 Specific loss w.r.t $\boldsymbol{\omega}$ and non-local parameter $\boldsymbol{\epsilon}$

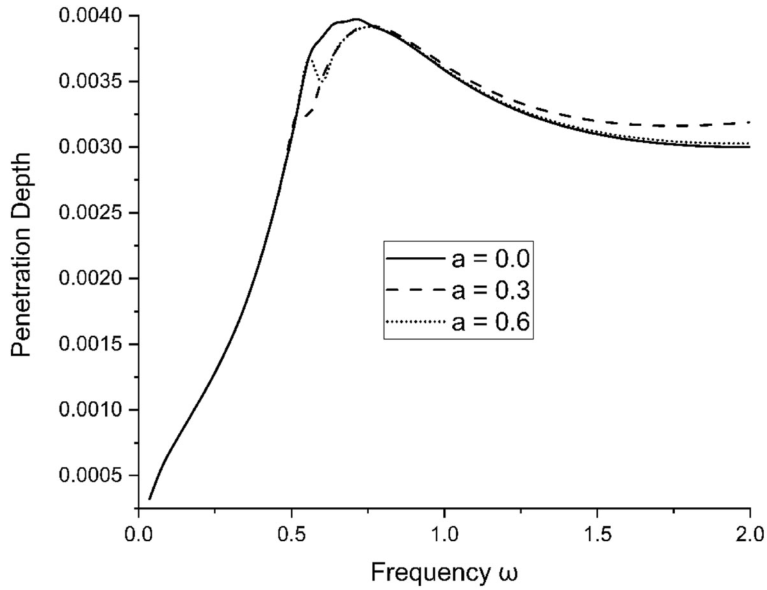

Fig. 13 Penetration depth w.r.t ***ω*** and fractional order heat transfer parameter ***a***

Nomenclature

δ_{ij} Kronecker delta
t_0 the pulse rise time
w lateral deflection of the beam
K_{ij} thermal conductivity
T_0 reference temperature
t_{ij} stress tensors
e_{ij} strain tensors
u_i displacement components
β_{ij} thermal elastic coupling tensor
ρ medium density
C_E specific heat
T temperature change
I moment of inertia of cross-section
t time
E_i intensity tensor of the electric field
m_e mass of the electron
t_e electron collision time
c_{ijkl} elastic parameters
M_T thermal moment of inertia

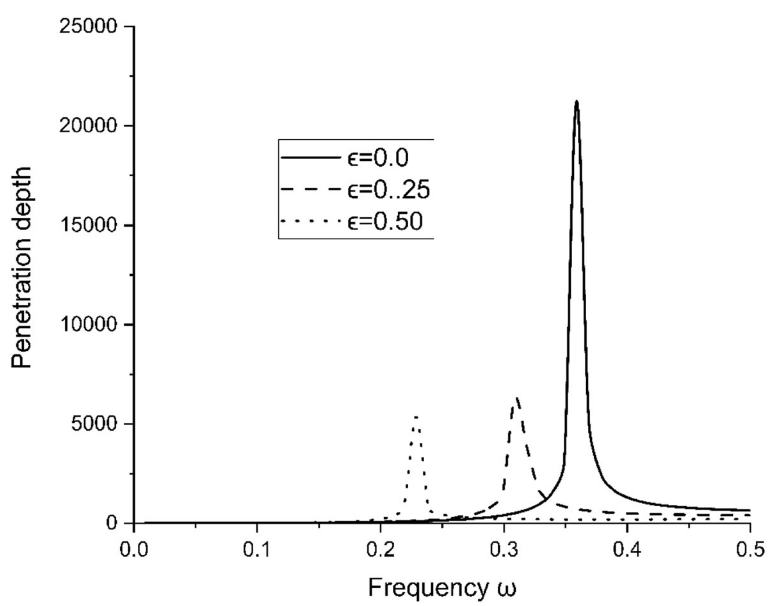

Fig. 14 Penetration depth w.r.t ***ω*** and Hall current parameter ***m***

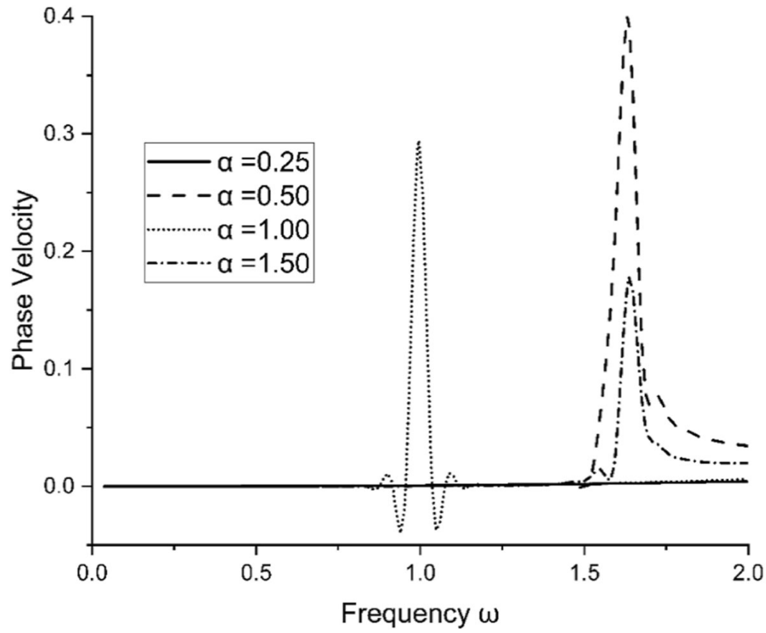

Fig. 15 Penetration depth w.r.t $\boldsymbol{\omega}$ and two temperature parameter $\boldsymbol{a}$

$\beta_1 M_T$ thermal moment of the beam
ϕ conductive temperature
μ_0 magnetic permeability
α_{ij} linear thermal expansion coefficient
a_{ij} two-temperature parameter
m Hall effect parameter$m = \omega_e t_e = \frac{\sigma_0 \mu_0 H_0}{e n_e}$
λ_i pyromagnetic coefficient
τ_q phase lags of the heat flux
τ_T phase lags of the temperature gradient
J_j conduction current density tensor
ε_{ilr} permutation symbol
H_r magnetic strength
e charge of the electron

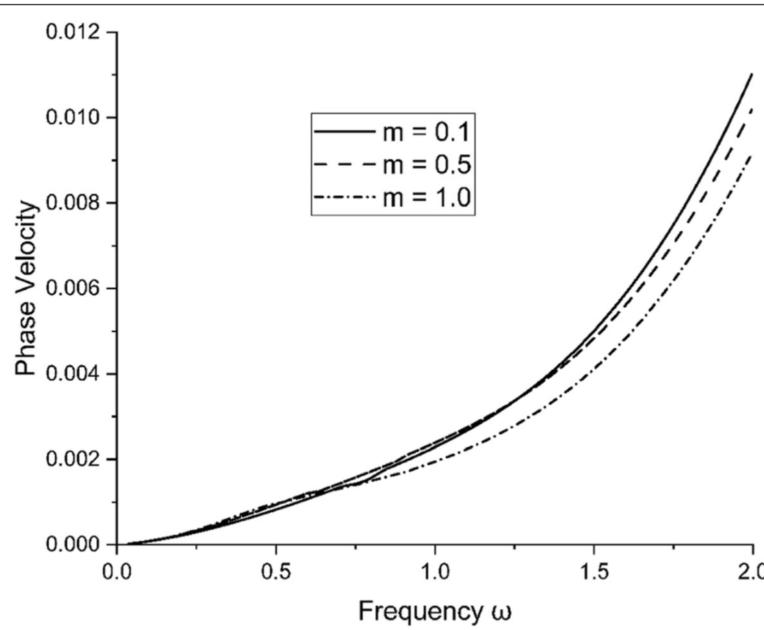

Fig. 16 Penetration depth w.r.t $\boldsymbol{\omega}$ and non-local parameter $\boldsymbol{\epsilon}$

n_e electron number density
σ_0 electrical conductivity and $=\sigma_0 = \frac{n_e e^2 t_e}{m_e}$
τ_v phase lags of the thermal displacement
K^*_{ij} materialistic constant
$t_{ij}(x)$ non-local stress tensor
$\sigma_{ij}(x)$ local stress tensor
ϵ nonlocal parameter
a internal characteristic length
e_0 constant characterizes the nonlocal effect of material
d_n coefficient of electronic deformation
α_T coefficient of linear thermal expansion
λ, μ Lame's elastic constants
N carrier density
D_E carrier diffusion coefficients
τ photo-generated carrier lifetime
E_g energy gap of the semiconductor parameter
$\kappa = \frac{\partial N_0}{\partial T}$ coupling parameter for thermal activation
N_0 carrier concentration at equilibrium position
s_0 velocity of recombination on the surface
M Hartmann number or magnetic parameter for semiconductor elastic medium

Abbreviations
TPL: Three-phase lag; 2T: Two temperatures; FOT: Fractional order theory; CLD: Coupled-longitudinal displacement; CT: Coupled thermal; CCD: Coupled carrier density; CTD: Coupled transverse displacement; TIT: Transversely isotropic thermoelastic; SPL-FOT: Single-phase lag FOT; GN: Green-Naghdi; TPL-FOT: Three-phase lag FOT; DPL-FOT: Dual-phase lag FOT; 2-D: Two-dimensional

Acknowledgements
Not applicable

Authors' contributions
Iqbal Kaur: idea formulation, conceptualization, formulated strategies for mathematical modeling, methodology refinement, formal analysis, validation, writing—review and editing. *Kulvinder Singh*: conceptualization, effective literature review, experiments, simulation, investigation, methodology, software, supervision, validation, visualization, writing—original draft. Both authors read and approved the final manuscript.

Funding
No fund/grant/scholarship has been taken for the research work.

Availability of data and materials
For the numerical results, cobalt material has been taken for thermoelastic material from Mahdy et al. (2020).

Declarations

Competing interests
The authors declare that they have no conflict of interest.

Author details
[1]Department of Mathematics, Government College for Girls, Palwal, Kurukshetra, Haryana, India. [2]Kurukshetra University Kurukshetra, Kurukshetra, Haryana, India.

Received: 20 May 2021 Accepted: 13 September 2021
Published online: 26 September 2021

References

Abbas, I. A., & Marin, M. (2018). Analytical solutions of a two-dimensional generalized thermoelastic diffusions problem due to laser pulse. *Iran J Sci Technol Trans Mech Eng*, *42*(1), 57–71 https://doi.org/10.1007/s40997-017-0077-1.

Ali, H., Jahangir, A., & Khan, A. (2020). Reflection of waves in a rotating semiconductor nanostructure medium through torsion-free boundary condition. *Ind J Phys*, *94*(12), 2051–2059 https://doi.org/10.1007/s12648-019-01652-y.

Alshaikh, F. (2020). Mathematical modeling of photothermal wave propagation in a semiconducting medium due to L-S theory with diffusion and rotation effects. *Mech Based Des Struct Mach*, 1–16 https://doi.org/10.1080/15397734.2020.1776620.

Bhatti, M. M., Ellahi, R., Zeeshan, A., Marin, M., & Ijaz, N. (2019). Numerical study of heat transfer and Hall current impact on peristaltic propulsion of particle-fluid suspension with compliant wall properties. *Mod Phys Lett B*, *33*(35), 1950439 https://doi.org/10.1142/S0217984919504396.

Bhatti, M. M., & Abdelsalam, S. I. (2020). Thermodynamic entropy of a magnetized Ree-Eyring particle-fluid motion with irreversibility process: a mathematical paradigm. *ZAMM J Appl Math Mech* https://doi.org/10.1002/zamm.202000186, *101*(6).

Bhatti, M. M., Elelamy, A. F., Sait, M. S., & Ellahi, R. (2020). Hydrodynamics interactions of metachronal waves on particulate-liquid motion through a ciliated annulus: application of bio-engineering in blood clotting and endoscopy. *Symmetry*, *12*(4), 532–547 https://doi.org/10.3390/sym12040532.

Bhatti, M. M., Phali, L., & Khalique, C. M. (2021). Heat transfer effects on electro-magnetohydrodynamic Carreau fluid flow between two micro-parallel plates with Darcy–Brinkman–Forchheimer medium. *Arch Appl Mech*, *91*(4), 1683–1695 https://doi.org/10.1007/s00419-020-01847-4.

A. Cemal Eringen. (2004). Nonlocal continuum field theories. (A. C. Eringen, Ed.). New York: Springer New York. https://doi.org/10.1007/b97697

Eringen, A. C. (1974). Theory of nonlocal thermoelasticity. *Int J Eng Sci*, *12*(12), 1063–1077 https://doi.org/10.1016/0020-7225(74)90033-0.

Eringen, A. C., & Edelen, D. G. B. (1972). On nonlocal elasticity. *Int J Eng Sci*, *10*(3), 233–248 https://doi.org/10.1016/0020-7225(72)90039-0.

Golewski, G. L. (2021). On the special construction and materials conditions reducing the negative impact of vibrations on concrete structures. *Mater Today Proc* https://doi.org/10.1016/j.matpr.2021.01.031.

Kaur, I., & Lata, P. (2019a). Effect of hall current on propagation of plane wave in transversely isotropic thermoelastic medium with two temperature and fractional order heat transfer. *SN Appl Sci*, *1*(8) https://doi.org/10.1007/s42452-019-0942-1.

Kaur, I., & Lata, P. (2019b). Rayleigh wave propagation in transversely isotropic magneto-thermoelastic medium with three-phase-lag heat transfer and diffusion. *Int J Mech Mater Eng*, *14*(1) https://doi.org/10.1186/s40712-019-0108-3.

Kaur, I., & Lata, P. (2020). Stoneley wave propagation in transversely isotropic thermoelastic medium with two temperature and rotation. *GEM Int J Geomath*, *11*(1), 1–17 https://doi.org/10.1007/s13137-020-0140-8.

Kaur, I., Lata, P., & Singh, K. (2020a). Reflection of plane harmonic wave in rotating media with fractional order heat transfer. *Adv Mater Res*, *9*(4), 289–309.

Kaur, I., Lata, P., & Singh, K. (2020b). Reflection and refraction of plane wave in piezo-thermoelastic diffusive half spaces with three phase lag memory dependent derivative and two-temperature. *Waves Random Complex Media*, 1–34 https://doi.org/10.1080/17455030.2020.1856451.

Lata, P., Kaur, I., & Singh, K. (2021). Reflection of plane harmonic wave in transversely isotropic magneto-thermoelastic with two temperature, rotation and multi-dual-phase lag heat transfer. *Lect Notes Netw Syst*, *140* https://doi.org/10.1007/978-981-15-7130-5_42.

Lata, P., & Kaur, I. (2018). Effect of hall current in Transversely Isotropic magneto thermoelastic rotating medium with fractional order heat transfer due to normal force. *Adv Mater Res (South Korea)*, *7*(3), 203–220 https://doi.org/10.12989/amr.2018.7.3.203.

Lata, P., & Kaur, I. (2019). Plane wave propagation in transversely isotropic magneto-thermoelastic rotating medium with fractional order generalized heat transfer. *Struct Monit Maintenance*, *6*(3), 191–218 https://doi.org/10.12989/smm.2019.6.3.191.

Lim, C. C., Pimbley, J. M., Schmeiser, C., & Schwendeman, D. W. (1992). Rotating Waves for Semiconductor Inverter Rings. *SIAM J Appl Math*, *52*(3), 676–690 https://doi.org/10.1137/0152037.

Lotfy, K. (2017). A novel solution of fractional order heat equation for photothermal waves in a semiconductor medium with a spherical cavity. *Chaos Solitons Fractals*, *99*, 233–242 https://doi.org/10.1016/j.chaos.2017.04.017.

Lotfy, K., El-Bary, A. A., Hassan, W., & Ahmed, M. H. (2020). Hall current influence of microtemperature magneto-elastic semiconductor material. *Superlattice Microst*, *139*, 106428 https://doi.org/10.1016/j.spmi.2020.106428.
Mahdy, A. M. S., Lotfy, K., Ahmed, M. H., El-Bary, A., & Ismail, E. A. (2020). Electromagnetic Hall current effect and fractional heat order for microtemperature photo-excited semiconductor medium with laser pulses. *Results Phys*, *17*, 103161 https://doi.org/10.1016/j.rinp.2020.103161.
Marin, M. (2010). Some estimates on vibrations in thermoelasticity of dipolar bodies. *J Vib Control*, *16*(1), 33–47 https://doi.org/10.1177/1077546309103419.
Marin, M., Vlase, S., & Paun, M. (2015). Considerations on double porosity structure for micropolar bodies. *AIP Adv*, *5*(3), 037113 https://doi.org/10.1063/1.4914912.
Marin, M. (1996). Generalized solutions in elasticity of micropolar bodies with voids. *Rev Acad Canaria Cienc*, *8*(1), 101–106.
Marin, M., Craciun, E. M., & Pop, N. (2020). Some results in Green – Lindsay thermoelasticity of bodies with dipolar structure. *Mathematics*, 1–12 https://doi.org/10.3390/math8040497.
Marin, M., Craciun, E.-M., & Pop, N. (2016). Considerations on mixed initial-boundary value problems for micropolar porous bodies. *Dyn Syst Appl*, *25*, 175–195.
Othman, M. I. A., & Abd-Elaziz, E. M. (2019). Effect of initial stress and Hall current on a magneto-thermoelastic porous medium with microtemperatures. *Ind J Phys*, *93*(4), 475–485 https://doi.org/10.1007/s12648-018-1313-2.
Pandey, P., Das, S., Craciun, E.-M., & Sadowski, T. (2021). Two-dimensional nonlinear time fractional reaction–diffusion equation in application to sub-diffusion process of the multicomponent fluid in porous media. *Meccanica*, *56*(1), 99–115 https://doi.org/10.1007/s11012-020-01268-1.
Tang, F., & Song, Y. (2018). Wave reflection in semiconductor nanostructures. *Theor Appl Mech Lett*, *8*(3), 160–163 https://doi.org/10.1016/j.taml.2018.03.003.
Taye, I. M., Lotfy, K., El-Bary, A. A., Alebraheem, J., & Asad, S. (2021). The hyperbolic two temperature semiconducting thermoelastic waves by laser pulses. *Comput Mater Contin*, *67*(3), 3601–3618 https://doi.org/10.32604/cmc.2021.015223.
Zhang, L., Bhatti, M. M., Marin, M., & Mekheimer, K. S. (2020a). Entropy analysis on the blood flow through anisotropically tapered arteries filled with magnetic zinc-oxide (ZnO) nanoparticles. *Entropy*, *22*(10) https://doi.org/10.3390/E22101070.
Zhang, L., Bhatti, M. M., & Michaelides, E. E. (2021). Electro-magnetohydrodynamic flow and heat transfer of a third-grade fluid using a Darcy-Brinkman-Forchheimer model. *Int J Numerical Methods Heat Fluid Flow*, *31*(8), 2623–2639 https://doi.org/10.1108/HFF-09-2020-0566.
Zhang, P., Han, S., Golewski, G. L., & Wang, X. (2020b). Nanoparticle-reinforced building materials with applications in civil engineering. *Adv Mech Eng*, *12*(10), 168781402096543 https://doi.org/10.1177/1687814020965438.

Publisher's Note

Springer Nature remains neutral with regard to jurisdictional claims in published maps and institutional affiliations.